Desalination and Water Treatment
www.deswater.com

doi: 10.5004/dwt.2017.21731

100 (2017) 151–159
December

Cu^{2+} adsorption onto sulfonated polyimide membrane: an experimental study

Sensen Xuan, Shuang Zhu, Yongjie Zhu, Yuqin Zhou, Pan Yang, Yang Pu, Hongping Zhang, Yaping Zhang*

Engineering Research Center of Biomass Materials, Ministry of Education, Southwest University of Science and Technology, Mianyang 621010, China, email: zhangyaping@swust.edu.cn (Y. Zhang)

Received 11 June 2017; Accepted 25 November 2017

ABSTRACT

Sulfonated polyimide (SPI) was synthesized by polycondensation and then coated to be the membrane for adsorption of Cu^{2+}. The chemical structure before and after adsorption was characterized by using FT-IR spectra. The morphology and element of SPI membrane surface were scanned by using SEM-EDX. The thermal stability was demonstrated by using TGA. Effects of initial pH value and concentration of the feed liquid together with adsorption time and temperature on the adsorption of Cu^{2+} have been studied respectively. The optimum pH value for adsorption of Cu^{2+} onto SPI membrane is 4.7. The adsorption capacity firstly increases with initial concentration of feed liquid, and then the adsorption equilibrium is gradually achieved when the initial concentration rises to be 40 mg L^{-1}. The adsorption of Cu^{2+} onto SPI membrane is in accordance with Langmuir isotherm model. Under the optimum adsorption conditions, Cu^{2+} adsorption capacity onto SPI membrane achieves 23.46 mg g^{-1}. When the adsorption time is controlled to be around 2 h, the adsorption kinetic equilibrium can be reached, and the adsorption process is consistent with the pseudo-first-order kinetic model. Besides, the washout rate of Cu^{2+} from SPI membrane after four-time adsorption-desorption recycle maintains as high as around 90%. As a result, SPI membrane is potential to treat the wastewater containing low concentration of Cu^{2+}.

Keywords: SPI membrane; Adsorption; Desorption; Copper ion

1. Introduction

With the rapid development of metal processing industry, more and more copper ions go into water environment to produce the industrial wastewater. The existence of excessive amounts of copper ions in water may cause serious problems for local flora and fauna, and excessive intake of copper ions by humans may lead to the damage of stomach, liver or kidney, even cancer [1–3]. Therefore, it is necessary to remove exceeded copper ions in water environment.

At present, there are many methods to treat wastewater containing copper ions, such as ion exchange [4–7], chemical precipitation [8–11], membrane separation [12–14] and adsorption [15–19]. Among these methods, the adsorption process has attracted more and more attention due to its simple operation, cost-effective, easy maintenance and high efficiency, etc. In general, the adsorption resins are used to study the adsorption of copper ions. For an instance, the polymer derivations of poly (styrene-alt-maleic anhydride) were reported to be efficient for removal of Cu^{2+} [20]. However, most adsorption resins are prepared as powders or granulars, inevitably leading to some disadvantages such as the compaction and recycling difficulty. One of the effective strategies to overcome such problems is membrane adsorption. That is, to prepare the adsorbent as membrane. Thus, the subsequent recovery and re-use of the membrane adsorbent are very convenient. For example, hybrid polymer membranes with embedded functional nanoadsorbent particles showed marked ability to adsorb Cu^{2+}, Ag^{+} and Pb^{2+} [21]. A novel porous membrane adsorbent polyethyleneimine/sodium alginate (PEI/SA) by immobilizing PEI with SA was reported to be promising for removal of Cu^{2+} [22]. These results indicate that the membrane adsorption method does have a great potential in the treatment of wastewater containing low concentration of Cu^{2+}.

*Corresponding author.

Sulfonated polyimide (SPI) has good membrane-forming property, high mechanical strength, excellent thermal and chemical stability [23–26]. SPI membrane has been widely used in all vanadium redox flow battery [27,28], hydrogen-oxygen fuel cell [29,30] and direct methanol fuel cell [31,32]. However, application of SPI membrane in the treatment of wastewater containing heavy metal ions has not been reported yet to the best of our knowledge. The advantages of SPI membrane are as the following: Firstly, there is a large number of $–SO_3H$ groups in SPI membrane, causing copper ions to be removed through the ion exchange accordingly. Secondly, sulfonated diamine was used as a monomer to synthesize SPI and the complex post-sulfonation process is avoided, and the degree of sulfonation can be controlled easily. Thirdly, compared with the porous membrane reported by Lin et al. [33], the preparation process of SPI membrane is simple, fast and green. In addition, the price of SPI membrane is cheaper than the adsorption resin reported by Cui et al. [34].

Consequently, in this work, SPI membrane with the degree of sulfonation of 50% was prepared and characterized firstly, and then it was used as an adsorbent to treat the simulated wastewater containing low concentration of Cu^{2+}. Effects of initial concentration and pH value of the feed liquid together with adsorption temperature and time were investigated respectively to obtain the optimum operation parameters. In addition, the desorption experiments were also conducted to verify the recyclability of as-prepared SPI membrane adsorbent.

2. Materials and methods

2.1. Materials

$CuSO_4·5H_2O$ was purchased from Guangdong Guanghua Chem. Co., China. 1, 4, 5, 8-naphthalenetetra-carboxylic dianhydride (NTDA) was bought from Beijing Multi. Tech. Co., China. 4, 4′-oxydianiline (ODA) was purchased from Beshine Chem. Co., China. *m*-cresol was purchased from Shanghai Kefeng Chem. Co., China. 4, 4′-diamino-biphenyl 2,2′-disulphonic acid (BDSA) was commercially obtained from Quzhou Rainful Chem. Co., China. 2-(4-aminophenyl)-5-aminobenzimidazole (APABI) was purchased from Shanghai Jingrui Industry and Trade. Co., China. Triethylamine (TEA) and other reagents were obtained from Chengdu Kelong Chem. Reagent Co., China. All chemical regents were used as received.

2.2. Preparation of SPI membrane

The TEA-type SPI was prepared from NTDA, BDSA, ODA and APABI according to the polycondensation method as presented by Zhang et al. [35]. The typical preparation process was as follows: Put 2.80 g of BDSA, 5.2 mL of TEA and 110 mL of *m*-cresol in a three-necked flask with temperature controlling device, magnetic stirring and condenser pipe under the protection of high purity N_2. Add 0.90 g of APABI, 0.80 g of ODA, 4.32 g of NTDA as well as 3.92 g of benzoic acid and stir them vigorously. Keep the reaction for 4 h at 80°C, and then maintain the reaction for 20 h at 180°C. Subsequently, cool down to 80°C, add 5.0 mL of *m*-cresol and continue to stir about five minutes, then the TEA-type SPI was obtained after pouring them into acetone. Wash TEA-type SPI several times using acetone and dry it at 40°C in the vacuum chamber. The TEA-type SPI membrane was prepared by coating its *m*-cresol solutions (7 % w/V) onto a clean glass plate evenly and drying it at 60°C for 24 h, then peel off the membrane. Later, the TEA-type SPI membrane was immersed into 1.0 mol L^{-1} H_2SO_4 for 24 h until the TEA-type SPI membrane was protonated. Then the H-type SPI membrane, namely, SPI membrane in this work, was washed several times with deionized water to remove the excessive sulfuric acid and dried at 40°C in a vacuum chamber. The synthesis schematic of SPI is shown in Fig. 1.

2.3. Characterization of SPI membrane

Nicolet-6700 FT-IR spectrometer (Thermoelectric Instrument Co., USA) at the wavenumber of 4000–600 cm^{-1} and over the resolution of 8 cm^{-1} was used to analysis the structure of SPI membrane. SEM-EDX system (Ultra55, Zeiss Instrument Co., Germany) was utilized to observe the morphology and the element at the surface of SPI membrane. Thermogravimetic analysis (TGA) (STA449C, Netzsch Instrument Co., Germany) was used to analyze the thermal stability at the heating temperature of 25–700°C and heating rate of 10°C min^{-1} in nitrogen atmosphere.

2.4. Adsorption processes

Add 50 mL of aqueous Cu^{2+} solution and 0.050 g of SPI membrane into a 50 mL beaker. Several adsorption experiments were conducted as below:

In order to study the effect of initial pH value of the feed liquid, fix the concentration of Cu^{2+} as 40 mg L^{-1}, adjust the initial pH value of feed liquid to be 2.0, 2.9, 3.8, 4.7 and 5.6 with sodium hydroxide (1.0 mol L^{-1}) and sulfuric acid (1.0 mol L^{-1}) solutions. The adsorption was carried out at 30°C, and the adsorption time was set as 2 h.

In order to study the effect of initial concentration of the feed liquid, fix the initial pH value as 4.7, change the initial Cu^{2+} concentration to be 4, 8, 12, 16, 20, 24, 32, 40, 55, 70, 85 and 100 mg L^{-1} respectively. The adsorption was carried out at 30°C, and the adsorption time was set as 2 h.

In order to study the effect of adsorption time, fix the initial pH and concentration of the feed liquid as 4.7 and 40 mg L^{-1} respectively, change the adsorption time to be 10, 20, 30, 40, 50, 60, 120 and 240 min individually. The adsorption was carried out at 30°C.

In order to study the effect of adsorption temperature, fix the initial pH and concentration of the feed liquid as 4.7 and 40 mg L^{-1} respectively, and the adsorption time was set to be 2 h, then change the adsorption temperature to be 20, 25, 30, 35 and 40°C individually.

Both the adsorption capacity and the removal percentage of Cu^{2+} are important indexes to estimate the adsorption performance. The adsorption capacity q (mg g^{-1}) is calculated using Eq. (1).

$$q = \frac{(C_0 - C_e) \times V}{m} \tag{1}$$

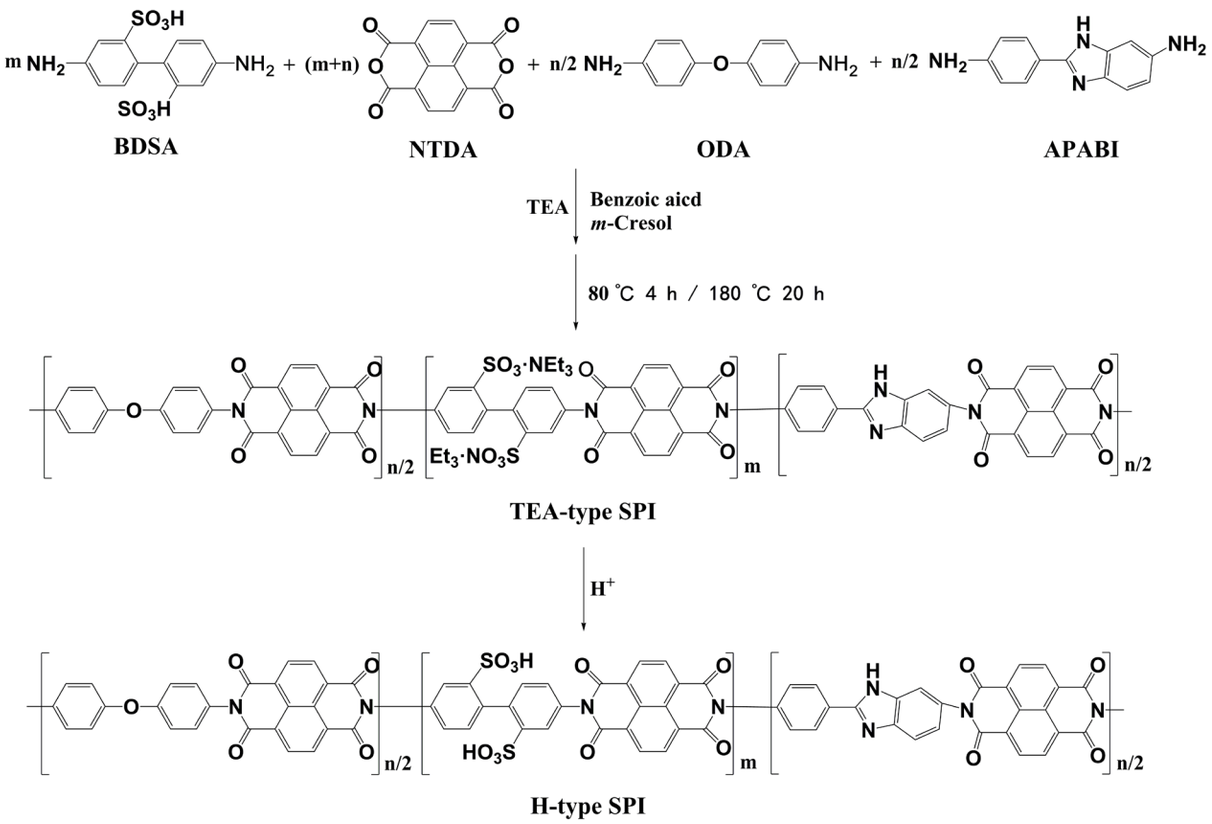

Fig. 1. Synthesis of SPI membrane.

where m (g) is the mass of SPI membrane, V (L) is the volume of feed liquid containing Cu^{2+}, C_0 and C_e (mg L^{-1}) are the concentration of Cu^{2+} measured by using atomic adsorption spectrophotometer (AA700, PerkinElmer Inc., USA) at the beginning and equilibrium of adsorption, respectively.

To reduce the experimental error, all experiments were performed three times and the average values were adopted, and the maximum error was less than ±5%.

The constant of adsorption equilibrium K_d is calculated by using Eq. (2):

$$\ln K_d = \frac{\Delta S}{R} - \frac{\Delta H}{RT} \tag{2}$$

where R is the constant of ideal gas (8.314 J K^{-1} mol^{-1}), and T is Kelvin temperature (K). ΔH is the molar adsorption enthalpy change (kJ mol^{-1}) and ΔS is the molar adsorption entropy change (J K^{-1} mol^{-1}), both of which can be evaluated by the slope and intercept from the line related $\ln K_d$ and $1/T$ (K^{-1}) respectively.

The molar adsorption Gibbs free energy change ΔG (kJ mol^{-1}) is calculated by using Eq. (3):

$$\Delta G = \Delta H - T\Delta S \tag{3}$$

During the desorption process, the sulfuric acid solution (1.0 mol L^{-1}) was used as an eluent. The SPI membrane reaching adsorption equilibrium was eluted several times. Then the concentration of Cu^{2+} in the eluent was measured. The elution rate D (%) is computed by using Eq. (4) as the following:

$$D = \frac{C_D \times V_D}{q_e m} \times 100\% \tag{4}$$

where q_e (mg g^{-1}) is the equilibrium adsorption capacity of Cu^{2+} onto SPI membrane, C_D (mg L^{-1}) is the concentration of Cu^{2+} in the filtrate after elution, and V_D (L) is the volume of eluted liquid.

3. Results and discussion

3.1. FT-IR analysis

The chemical structure of SPI membrane before and after adsorption was studied by using FT-IR spectra, and the results are shown in Fig. 2. For SPI membrane before adsorption, the symmetrical stretching vibration and asymmetric stretching vibration of C=O at 1670 cm^{-1} and 1711 cm^{-1} are observed, respectively. The peak at 1346 cm^{-1} is attributed to the asymmetric stretching vibration of C-N-C. Peaks at 1031, 1099 and 1249 cm^{-1} are the stretching vibration of $–SO_3H$. The adsorption peak at 1197 cm^{-1} is the characteristic peak of –O–. As expected, the peak at around 1780 cm^{-1} ascribed to polyamic acid is not detected, verifying the complete imidization of SPI. These results demonstrate that SPI membrane has been synthesized and prepared successfully. In addition, the characteristic peak of $–SO_3H$ has a lit-

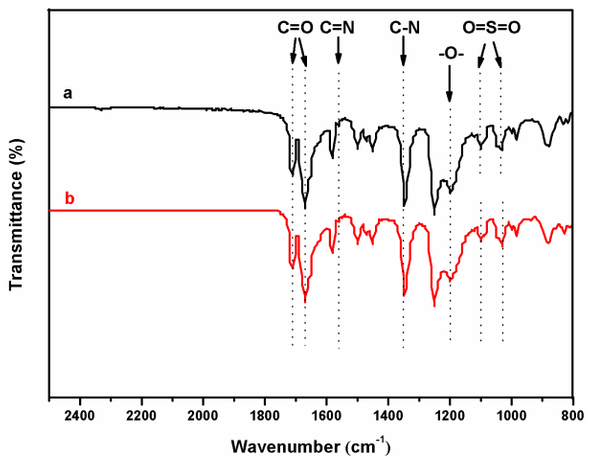

Fig. 2. FTIR spectra of SPI membrane: a) before and b) after adsorption.

tle shift for SPI membrane after adsorption, which may be caused by the ion exchange between H^+ in SPI membrane and Cu^{2+} in the solution during the adsorption process [36].

3.2. SEM-EDX analysis

The SEM images and EDX spectra of the surfaces of initial and Cu^{2+} adsorbed SPI membrane are shown in Figs. 3a, b and Figs. 4a, b respectively. As can be seen from Figs. 3a, b, the initial SPI membrane surface is smooth and homogeneous even at 3.00 K magnification. In comparison, some light spots less than 1.0 μm exist in the SEM image of the surface of Cu^{2+} adsorbed SPI membrane, which are probably ascribed to the morphology of adsorbed Cu^{2+}. And such a deduction is demonstrated by the EDX spectra of SPI membrane after adsorption in Fig. 4b, where Cu element can be apparently observed. But Cu element can't be detected at the surface of SPI membrane before adsorption in Fig. 4a. Thus, it can be inferred that SPI membrane has the ability to adsorb Cu^{2+}, which is in agreement with the above-presented FT-IR results.

3.3. Thermal analysis

Both TGA and DTG curves of SPI membrane before and after adsorption are showed in Figs. 5a, b. Similarly with what was reported in the literature [35], there are three weight loss steps of SPI membrane (see Fig. 5a). The first stage is ranged from 25°C to 150°C because of the evaporation of water. In the second stage, the SPI membrane shows an obvious mass loss in the temperature range of 300–450°C, which is attributed to the decomposition of sulfonic acid groups. The third weight loss is observed beyond 550°C, which is considered to be the decomposition of the backbone of SPI membrane. Fig. 5b shows that the degradation temperature of sulfonic groups is above 300°C and the degradation temperature of the main chain of SPI membrane is higher than 550°C. As can be seen from Figs. 5a,b, the degradation temperature of sulfonic groups in SPI membrane after adsorption is lower than that before adsorption.

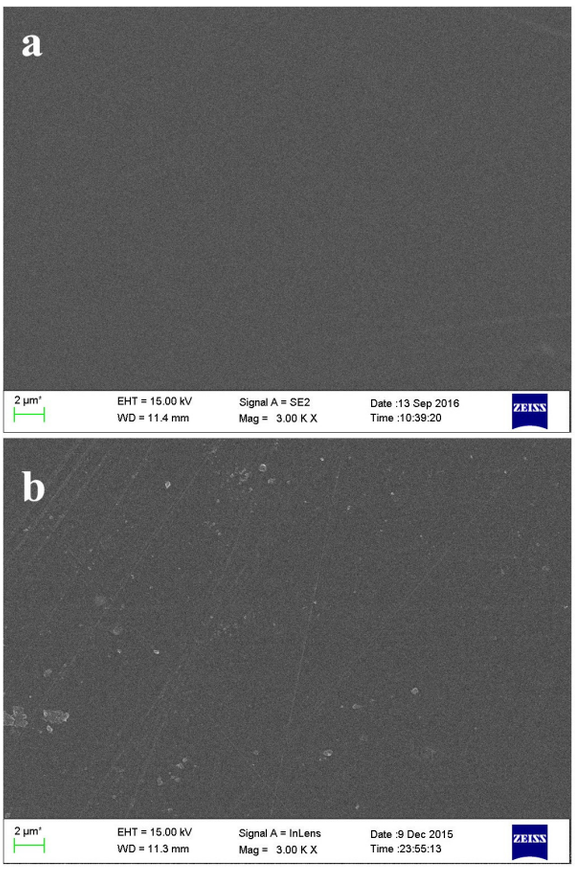

Fig. 3. SEM image of the surface of SPI membrane: a) before and b) after adsorption.

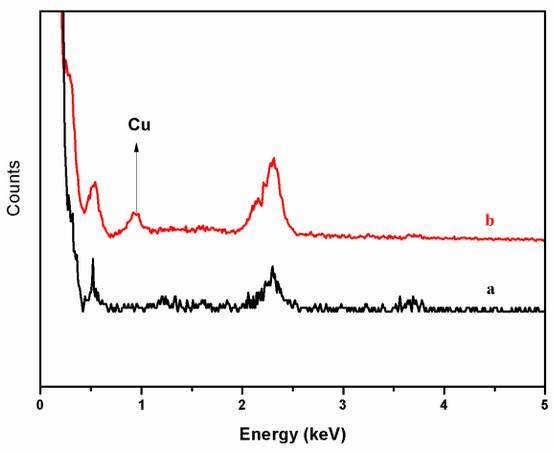

Fig. 4. EDX spectra of the surface of SPI membrane: a) before and b) after adsorption.

This is because that the interaction between H^+ and $(-SO_3)^-$ is the covalent bond, but the interaction between Cu^{2+} and $(-SO_3)^-$ is the ionic bond, and the energy of covalent bond is higher than that of ionic bond. Apparently, the degradation temperature of the main chain of SPI membrane after

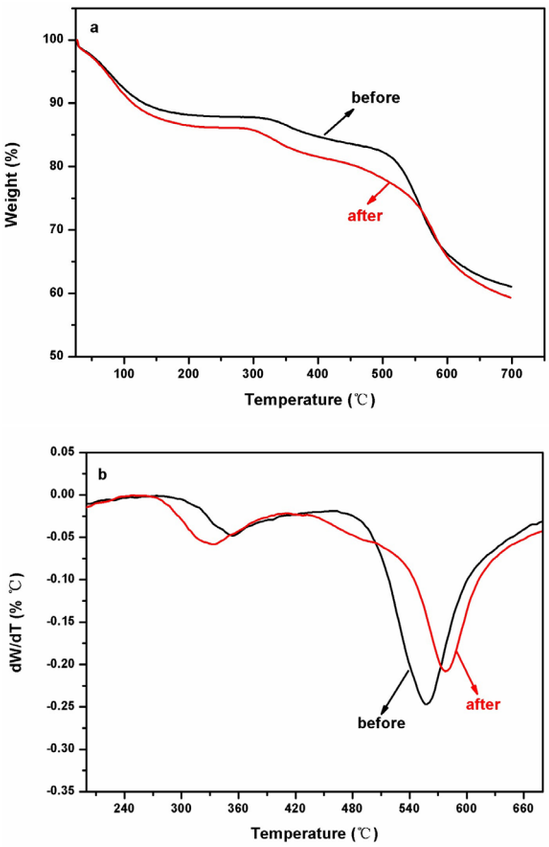

Fig. 5. a) TGA and b) DTG curves of SPI membrane before and after adsorption.

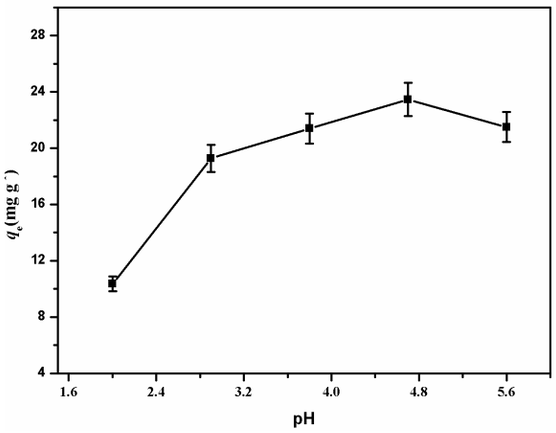

Fig. 6. Effect of initial pH value of the feed liquid on the adsorption capacity.

adsorption is higher than that before adsorption, the reason is possibly that the adsorption of Cu^{2+} in SPI membrane increases the interaction of the backbone of SPI membrane. All in all, the thermal stability of SPI membrane is mainly dependent on its sulfonic groups, and the sulfonic groups decompose above 300°C in this work, which is much higher than the adsorption temperature. Accordingly, the SPI membrane has extremely thermal stability to apply to the treatment of wastewater containing Cu^{2+}.

3.4. Effect of initial pH of the feed liquid

Fig. 6 shows the effect of initial pH value on the adsorption capacity. The adsorption capacity of SPI membrane increases with rising initial pH of the feed liquid when the initial pH ranges from 2.0 to 4.7, and the maximum adsorption capacity is about 23.46 mg g^{-1}, which is higher than the membrane adsorbents as reported by Ghaee et al. [37]. The reason may be that $–SO_3H$ groups in SPI membrane can improve the adsorbing capacity. However, the adsorption capacity of SPI membrane decreases with the increase of initial pH when the pH is larger than 4.7, and the adsorption capacity reaches the minimum when the pH is equal to around 5.8. The reasons are as follows: The acidity of the solution to be adsorbed is very high at low pH, and there are large quantities of H^+ and H_3O^+ in the solution. These ions compete with Cu^{2+}, which leads to the reduction of adsorption capacity of Cu^{2+} onto SPI membrane. Such a competitive effect is weakened and the adsorption capacity increases with rising pH, and then the adsorption capacity reaches the highest when the pH is 4.7. Afterwards, the gradually increased OH^- is disadvantageous to the adsorption of Cu^{2+} when the pH is higher than 4.7, resulting in the reduction of adsorption capacity. When the initial pH value is equal to or larger than 5.8, the product of the activity of Cu^{2+} and the square of the activity of OH^- is larger than the solubility product constant of $Cu(OH)_2$, so the participation $Cu(OH)_2$ is produced considering the concentration of Cu^{2+} is 40 mg L^{-1}. As a result, the adsorption experiment is ended at around 5.8 of initial pH value of the feed liquid.

3.5. Effect of initial concentration of the feed liquid

The adsorption of Cu^{2+} onto SPI membrane at the initial concentration ranged from 4 to 100 mg L^{-1} under initial pH of 4.7 was studied, and the results are shown in Fig. 7. As expected, the adsorption capacity firstly rises sharply and then changes little when increasing the initial concentration. The adsorption capacity gradually approaches its equilibrium value when the initial concentration is larger than 40 mg L^{-1}. This is because that Cu^{2+} has occupied the active site of SPI membrane gradually at higher initial concentration, approaching the adsorption equilibrium and constant adsorption consequently.

The experimental data were fitted by both Freundlich and Langmuir adsorption models as reported by Zhang et al. [38], and the results are shown in Figs. 8a, b. The parameters calculated from the fitting graphs by using Langmuir and Freundlich isotherms are listed in Table 1. As a correlation index of the adsorption isotherm, R^2 calculated by using Langmuir isotherm model is close to 1.0, which is much larger than that calculated by using Freundlich isotherm model. Therefore, Langmuir adsorption isotherm model is more suitable to express the adsorption behavior of Cu^{2+} onto SPI membrane. This means that the adsorption of Cu^{2+} onto SPI membrane is dominated by monolayer adsorp-

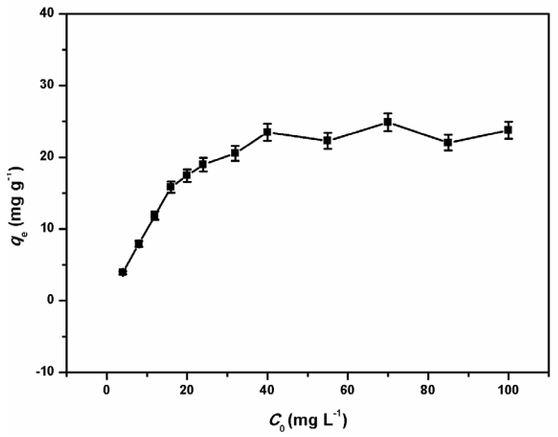

Fig. 7. Effect of initial concentration of the feed liquid on the adsorption capacity.

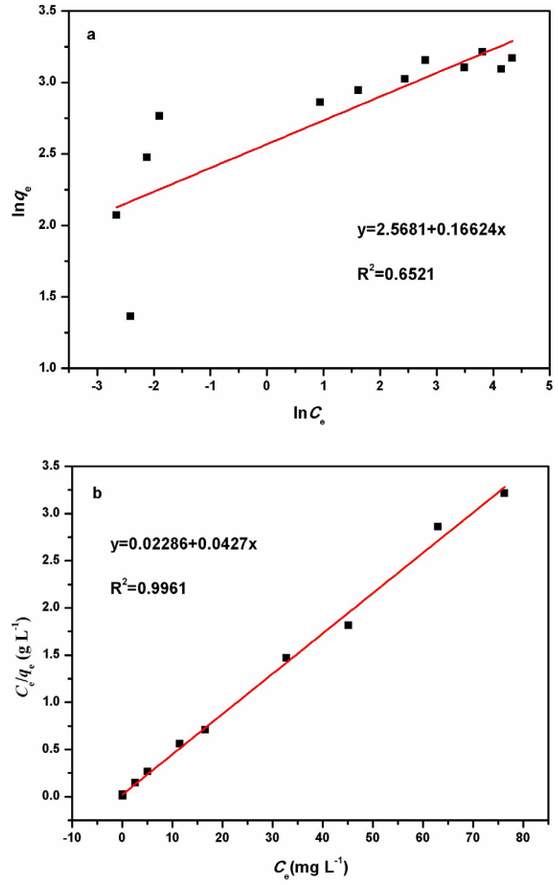

Fig. 8. Linear fitting by using the isotherm model: a) Freundlich and b) Langmuir.

tion. In addition, the q_m which is the theoretical single-layer saturated adsorption capacity of Cu^{2+} onto SPI membrane is fitted to be 23.42 mg g^{-1}, and it is very close to above q_e which is the actual single-layer saturated adsorption capacity of SPI membrane. Such a result verifies again that Langmuir adsorption isotherm model is suitable to describe the adsorption of Cu^{2+} onto SPI membrane.

Table 1
Isothermal fitting parameters of the adsorption

Parameter	Freundlich	Langmuir
q_m (mg g^{-1})		23.42
n	6.02	
K_F (mg^{1-n} L^n g^{-1})	13.04	
K_L (L mg^{-1})		1.87
R^2	0.65	0.99

3.6. Effect of adsorption time

The adsorption time has a great influence in the adsorption process. The dependency of adsorption time on the adsorption capacity is shown in Fig. 9. The adsorption capacity of Cu^{2+} onto SPI membrane increases rapidly as the elapsed time, then it rises slowly and reaches the adsorption equilibrium when the adsorption time is close to 120 min. This is because that the concentration of Cu^{2+} in the solution decreases gradually with the time extended, and the difference of concentration of Cu^{2+} in the adsorbent and liquid phase also reduces increasingly. This leads to the decrease of driving force of the adsorption, and the adsorption rate is slowed down until the system reaches the adsorption equilibrium. Based on such results, 120 min is chosen as the optimum adsorption time in subsequent adsorption experiments. The required time for Cu^{2+} adsorption onto SPI membrane to reach adsorption equilibrium in this work is shorter than Cu^{2+} adsorption in other reported adsorbents [39,40]. This may be the presence of a large number of vacant surface sites in SPI membrane for adsorption. To further analyze the kinetic adsorption behavior of Cu^{2+} onto SPI membrane, both pseudo-first-order and pseudo-second-order kinetic equations were used to fit the data of adsorption test as reported by Demiral and Güngör [41], and the results are shown in Figs. 10a, b and Table 2 respectively. It can be seen from Fig. 10 that the pseudo-second-order kinetic equation is more suitable to fit the experimental data in this work. Moreover, results in Table 2 show that the measured equilibrium adsorption capacity is close to that calculated by using pseudo-second-order kinetic equation, and the linear correlation coefficient achieves as high as close to 1.0. Therefore, the pseudo-second-order kinetic equation can fit the adsorption kinetics of Cu^{2+} onto SPI membrane well. In other words, both the adsorption time and the initial concentration of Cu^{2+} have some influences on the residue concentration of Cu^{2+} in the solution. Above kinetic adsorption results also indicate that the chemical adsorption plays a dominant role in the adsorption process.

3.7. Effect of adsorption temperature

Fig. 11 shows the effect of temperature on the adsorption of Cu^{2+} onto SPI membrane. As can be observed from Fig. 11, the adsorption capacity increases with rising temperature. That is, the elevated temperature can promote the adsorption of Cu^{2+} onto SPI membrane. It is probable

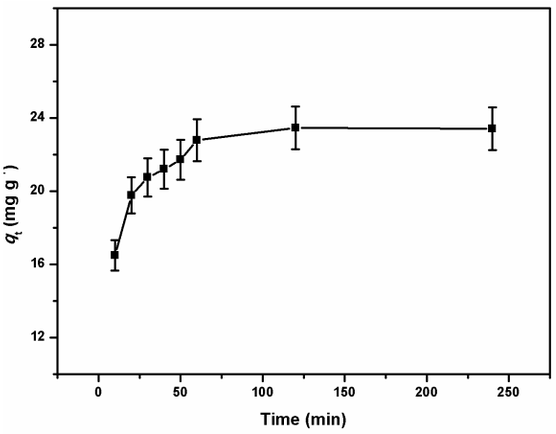

Fig. 9. Effect of adsorption time on the adsorption capacity.

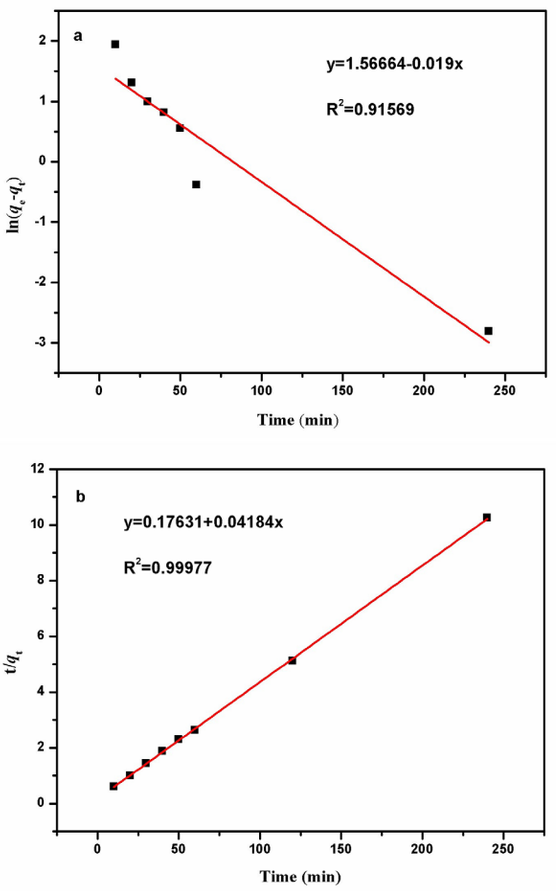

Fig. 10. Linear fitting by using the kinetic model: a) Pseudo-first-order and b) Pseudo-second-order.

that the increase of temperature can increase the number of active sites on the surface of adsorbent [42]. This indicates that the adsorption process is an endothermic process. However, in order to save the operation cost and increase the actual economic benefit, the adsorption process is suggested to be conducted at 30°C in the practical application, because the difference of the adsorption capacity at various temperature is very small when the temperature is higher than 30°C.

Table 2
Kinetic fitting parameters of the adsorption

Parameter	Pseudo-first-order	Pseudo-second-order
$q_{e,exp}$ (mg g^{-1})	23.46	
$q_{e,cal}$ (mg g^{-1})	4.79	23.90
K_1 (min^{-1})	0.02	
K_2 (g mg^{-1} min^{-1})		0.01
R^2	0.92	0.99

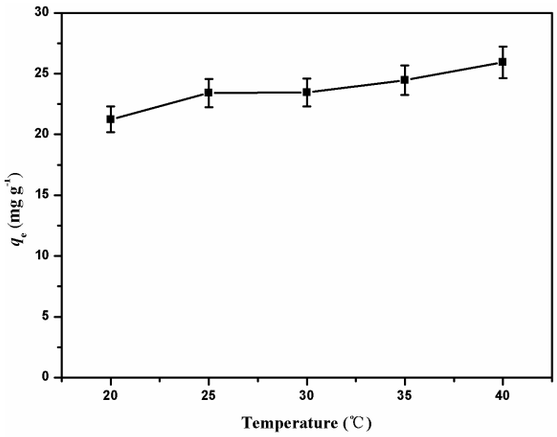

Fig. 11. Effect of temperature of the feed liquid on the adsorption capacity.

To further investigate the thermodynamic process of adsorption behavior, the following thermodynamic parameters were calculated according to Eqs. (3), (4) respectively: ΔH (kJ mol^{-1}), ΔS (J K^{-1} mol^{-1}) and ΔG (kJ mol^{-1}). The results are shown in Fig. 12, and the corresponding thermodynamic parameters are listed in Table 3. As shown in Table 3, the adsorption of Cu^{2+} onto SPI membrane is an endothermic and entropy-increased process. Such an adsorption can occur spontaneously under the laboratory condition since the molar Gibbs free energy is less than zero. Because the absolute value of molar Gibbs free energy increases with temperature, high temperature is beneficial to the increase of adsorption capacity and removal percentage of Cu^{2+}.

3.8. Desorption and recycle of SPI membrane

To research the reuse performance of SPI membrane as an adsorbent, several desorption experiments were carried out. It is found that the elution rate of Cu^{2+} can achieve higher than 90% when the eluent is sulfuric acid solution. The reason is as below: when the eluent is strong acid, there are a large quantity of H^+ in the elution liquid, and H^+ in the eluent exchanges with adsorbed Cu^{2+} onto SPI membrane during the elution process. Thus, the desorption effect is excellent when the eluent is sulfuric acid solution. As a

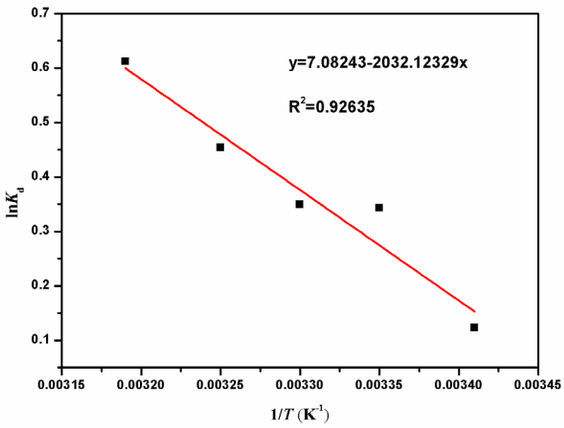

Fig. 12. Linear fitting of lnK_d versus 1/T.

Table 3
Thermodynamic parameters of the adsorption

Temperature (K)	ΔG (kJ mol^{-1})	ΔH (kJ mol^{-1})	ΔS (J K^{-1} mol^{-1})
293.15	–0.40		
298.15	–0.69		
303.15	–0.99	16.90	58.88
308.15	–1.28		
313.15	–1.58		

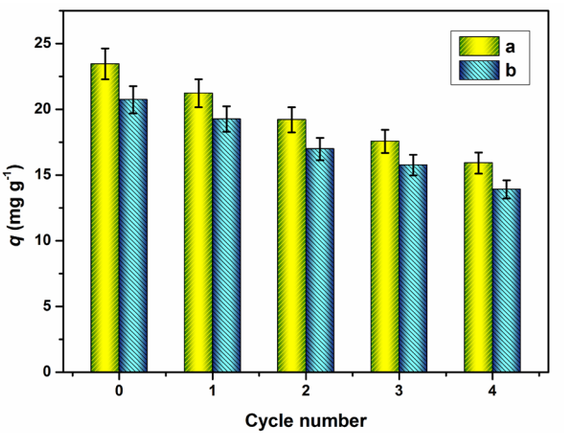

Fig. 13. Desorption performance of SPI membrane for adsorbing Cu^{2+}: a) adsorption capacity; b) elution capacity.

result, the sulfuric acid solution is chosen as the eluent to be used in subsequent repetitive desorption experiments.

Similar adsorption-desorption experiments were repeated four times, and the adsorption capacity and elution capacity were illustrated in Figs. 13a, b. Apparently, the adsorption capacity can reach 68% of that in the first time after four-time adsorption-desorption processes, and the elution rate maintains around 90%. These results demonstrate that SPI membrane has stable adsorption property, and it can be recycled as a consequence. But compared with other Cu^{2+} adsorbents such as novel ligand immobilized facial composite adsorbent [43], the regeneration performance of SPI membrane still needs to be improved, and this is under way in our lab.

4. Conclusions

In this work, SPI membrane was synthesized and prepared by using NTDA, BDSA, ODA and APABI as monomers. FT-IR spectra verify the success preparation of SPI membrane. SEM images illustrate the morphological integrity of as-prepared SPI membrane. EDX results demonstrate the adsorption of Cu^{2+} onto SPI membrane adsorbent. Various parameters including initial pH and concentration, adsorption time and temperature were studied individually. The optimum pH value is 4.7, and the adsorption equilibrium is reached when the adsorption time is 120 min. The adsorption capacity reaches saturation when the concentration of Cu^{2+} is equal to or higher than 40 mg L^{-1}. Results of adsorption isotherms show that the adsorption of Cu^{2+} onto SPI membrane belongs to monolayer adsorption in accordance with Langmuir model, and the theoretical monolayer adsorption capacity is 23.42 mg g^{-1}. The results of kinetic adsorption studies show that the adsorption of Cu^{2+} onto SPI membrane is in agreement with the pseudo-first-order kinetic equation, and the equilibrium adsorption capacity is consistent with the calculated value. The thermodynamic results show that the adsorption of Cu^{2+} onto SPI membrane is a spontaneous and endothermic process.

Elution experiments with sulfuric acid as the eluent show that the elution rate can reach up to 90%, and the repeated adsorption can be realized. All experimental results demonstrate that the as-prepared SPI membrane is very potential to be applied as an adsorbent for Cu^{2+}.

Next, we will design and optimize the structure and performance of SPI membrane to increase its cost performance. For example, design and optimize the species and structure of monomers to synthesize novel SPI membrane, introduce the porous structure to increase the specific surface area and improve the adsorption performance, and so on.

Acknowledgements

Financial support from National Key Scientific Projects for Decommissioning of Nuclear Facilities and Radioactive Waste Management (14zg6101) and Longshan Academic Talent Research Supporting Program of SWUST (17LZX402) is greatly acknowledged.

References

[1] H. Ma, O. Kökkılıç, K.E. Waters, The use of the emulsion liquid membrane technique to remove copper ions from aqueous systems using statistical experimental design, Miner. Eng., 107 (2017) 88–89.
[2] A.A. Moneer, A.A. Elshafei, M.M. Elewa, M.M. Naim, Removal of copper from simulated wastewater by electrocoagulation/floatation technique, Desal. Water Treat., 57 (2016) 48–49.

[3] J. Xu, Z. Qu, N. Yan, Y. Zhao, X. Xu, L. Li, Size-dependent nanocrystal sorbent for copper removal from water, Chem. Eng. J., 284 (2016) 565–570.
[4] T.B. Budak, Removal of heavy metals from wastewater using synthetic ion exchange resin, Asian. J. Chem., 25(8) (2013) 4207–4210.
[5] A.K.S. Clemens, A. Shishkin, P.A. Carlsson, M. Skoglundh, F.J. Martínezcasado, Z. Matěj, O. Balmes, H. Härelind, Reaction-driven ion exchange of copper into zeolite ssz-13, Acs Catal., 5(10) (2015) 6209–6218.
[6] S. Edebali, E. Pehlivan, Evaluation of chelate and cation exchange resins to remove copper ions, Powder Technol., 301 (2016) 520–525.
[7] C.E. Borba, E.A. Silva, S. Spohr, G.H.F. Santos, R. Guirardello, Ion exchange equilibrium prediction for the system Cu^{2+}–Zn^{2+}–Na^{+}, J. Chem. Eng. Data, 55(3) (2010) 1333–1341.
[8] L. Coudert, J.F. Blais, G. Mercier, P. Cooper, A. Janin, L. Gastonguay, Demonstration of the efficiency and robustness of an acid leaching process to remove metals from various CCA-treated wood samples, J. Environ. Manage., 132 (2014) 197–206.
[9] I. Giannopoulou, D. Panias, Differential precipitation of copper and nickel from acidic polymetallic aqueous solutions, Hydrometallurgy, 90(2–4) (2008) 137–146.
[10] S. Jiang, J. Qu, Y. Xiong, Removal of chelated copper from wastewaters by Fe^{2+}-based replacement-precipitation, Environ. Chem. Lett., 8(4) (2010) 339–342.
[11] D.H. Kim, M.C. Shin, H.D. Choi, C.I. Seo, K. Baek, Removal mechanisms of copper using steel-making slag: adsorption and precipitation, Desalination, 223 (2008) 283–289.
[12] Z.H. Cheng, X.S. Liu, M. Han, W. Ma, Adsorption kinetic character of copper ions onto a modified chitosan transparent thin membrane from aqueous solution, J. Hazard. Mater., 182 (2010) 408–415.
[13] B. Pośpiech, Separation of silver (I) and copper (II) from aqueous solutions by transport through polymer inclusion membranes with cyanex 471x, Sep. Sci. Technol., 47(9) (2012) 1413–1419.
[14] B. Pośpiech, W. Walkowiak, Separation of copper (II), cobalt (II) and nickel (II) from chloride solutions by polymer inclusion membranes, Sep. Purif. Technol., 57(3) (2007) 461–465.
[15] Z. Wang, G. Huang, C. An, L. Chen, J. Liu, Removal of copper, zinc and cadmium ions through adsorption on water-quenched blast furnace slag, Desal. Water Treat., 57(47) (2016) 22493–22506.
[16] M.T. Amin, A.A. Alazba, M. Shafiq, Adsorption of copper (Cu^{2+}) from aqueous solution using date palm trunk fibre: isotherms and kinetics, Desal. Water Treat., 57(47) (2016) 22454–22466.
[17] M.A. Kamal, T. Yasin, L. Reinert, L. Duclaux, Adsorptive removal of copper (II) ions from aqueous solution by silane cross-linked chitosan/PVA/TEOS beads: kinetics and isotherms, Desal. Water Treat., 57(9) (2016) 4037–4048.
[18] L.E. Fakir, M. Flayou, A. Dahchour, S. Sebbahi, F. Kifanisahban, S.E. Hajjaji, Adsorptive removal of copper (II) from aqueous solutions on phosphates: equilibrium, kinetics, and thermodynamics, Desal. Water Treat., 57(36) (2016) 17118–17127.
[19] V.V. Geetha, A.K. Misra, Equilibrium and kinetic studies on the adsorption of copper onto paddy straw powder, Desal. Water Treat., 57(28) (2016) 13081–13090.
[20] N. Samadi, R. Ansari, B. Khodavirdilo, Removal of copper ions from aqueous solutions using polymer derivations of poly (styrene-alt-maleic anhydride), Egyptian J. Petrol., 26(2) (2017) 375–389.
[21] K. Niedergall, D. Kopp, S. Besch, T. Schiestel, Mixed-matrix membrane adsorbers for the selective binding of metal ions from diluted solutions, Chem. Ing. Tech., 88(4) (2016) 437–446.
[22] X. Sun, J. Chen, Z. Su, Y. Huang, X. Dong, Highly effective removal of Cu(II) by a novel 3-aminopropyltriethoxysilane functionalized polyethyleneimine/sodium alginate porous membrane adsorbent, Chem. Eng. J., 290 (2016) 1–11.
[23] C. Genies, R. Mercier, B. Sillion, R. Petiaud, N. Cornet, G. Gebel, M. Pineri, Stability study of sulfonated phthalic and naphthalenic polyimide structures in aqueous medium, Polymer, 42(12) (2001) 5097–5105.
[24] Y. Yin, S. Hayashi, O. Yamada, H. Kita, K. Okamoto, Branched/crosslinked sulfonated polyimide membranes for polymer electrolyte fuel cells, Macromol. Rapid Comm., 26(9) (2005) 696–700.
[25] Y. Yin, Y. Suto, T. Sakabe, S. Chen, S. Hayashi, T. Mishima, O. Yamada, K. Tanaka, H. Kita, K. Okamoto, Water stability of sulfonated polyimide membranes, Macromolecules, 39(3) (2006) 1189–1198.
[26] Y. Yin, O. Yamada, K. Tanaka, K. Okamoto, On the development of naphthalene-based sulfonated polyimide membranes for fuel cell applications, Polym. J., 38(3) (2006) 197–219.
[27] L. Cao, Q. Sun, Y. Gao, L. Liu, H. Shi, Novel acid-base hybrid membrane based on amine-functionalized reduced graphene oxide and sulfonated polyimide for vanadium redox flow battery, Electrochim. Acta, 158 (2015) 24–34.
[28] X. Huang, Y. Pu, Y. Zhou, Y. Zhang, H. Zhang, In-situ and ex-situ degradation of sulfonated polyimide membrane for vanadium redox flow battery application, J. Membr. Sci., 526 (2017) 281–292.
[29] S. Faure, N. Cornet, G. Gebel, R. Mercier, M. Pineri, B. Sillion, Sulfonated polyimides as novel proton exchange membranes for H_2/O_2 fuel cells, J. Multi-Criteria Decision Anal., 3(1) (1997) 1–1.
[30] B. He, W.S.W. Ho, Synthesis and characterization of new sulfonated polyimide copolymers and blends as proton-exchange membranes for fuel cells, J. Environ. Eng. Manage., 18 (2008) 289–300.
[31] Y. Woo, S.Y. Oh, Y.S. Kang, B. Jung, Synthesis and characterization of sulfonated polyimide membranes for direct methanol fuel cell, J. Membr. Sci., 220(1–2) (2003) 31–45.
[32] F. Zhai, X. Guo, J. Fang, H. Xu, Synthesis and properties of novel sulfonated polyimide membranes for direct methanol fuel cell application, J. Membr. Sci., 296(1–2) (2007) 102–109.
[33] C.H. Lin, C.H. Gung, J.Y. Wu, S.Y. Suen, Cationic dye adsorption using porous composite membrane prepared from plastic and plant wastes, J. Taiwan Inst. Chem. E., 51 (2015) 119–126.
[34] L. Cui, Y. Wang, L. Gao, L. Hu, Q. Wei, B. Du, Removal of Hg (II) from aqueous solution by resin loaded magnetic β-cyclodextrin bead and graphene oxide sheet: Synthesis, adsorption mechanism and separation properties, J. Colloid Interf. Sci., 456 (2015) 42–49.
[35] Y. Zhang, J. Li, H. Zhang, S. Zhang, X. Huang, Sulfonated polyimide membranes with different non-sulfonated diamines for vanadium redox battery applications, Electrochim. Acta, 150 (2014) 114–122.
[36] Z. Li, X. Liu, The relationship between the changes of the infrared adsorption frequency and the electric effects and properties of the organic molecules, J. Baotou U. Iron Steel Tech., 15(2) (1996) 37–42.
[37] A. Ghaee, M. Shariaty-Niassar, J. Barzin, T. Matsuura, Effects of chitosan membrane morphology on copper ion adsorption, Chem. Eng. J., 165(1) (2010) 46–55.
[38] Y. Zhang, X. Wang, J. Liu, L. Wu, Removal of copper (Cu^{2+}) from water using novel hybrid adsorbents: kinetics and isotherms, J. Chem. Eng. Data, 58(5) (2013) 1141–1150.
[39] N. Bakhtiari, S. Azizian, S.M. Alshehri, N.L. Torad, V. Malgras, Y. Yamauchi, Study on adsorption of copper ion from aqueous solution by MOF-derived nanoporous carbon, Micropor. Mesopor. Mat., 217 (2015) 173–177.
[40] H.D. Ji, H.K. Ji, J.K. Hyeong, F.A. Rana, S. Koo, J.H. Young, Enhanced adsorption of aqueous copper (II) ions using dedoped poly-N-phenylglycine nanofibers, Chem. Eng. J., 277 (2015) 352–359.
[41] H. Demiral, C. Güngör, Adsorption of copper (II) from aqueous solutions on activated carbon prepared from grape bagasse, J. Clean. Prod., 124 (2016) 103–113.
[42] G.K. Incili, G.A. Aycık, Chemical modification of silica gel with synthesized Schiff base hydrazone derivative and application for preconcentration and separation of U(VI) ions from aqueous solutions, J. Radioanal. Nucl. Ch., 301(2) (2014) 417–426.
[43] M.R. Awual, A novel facial composite adsorbent for enhanced copper(II) detection and removal from wastewater, Chem. Eng. J., 266 (2015) 368–375.